Letters

IOP Publishing

Superconductor Science and Technology

Supercond. Sci. Technol. **34** (2021) 10LT01 (8pp)

https://doi.org/10.1088/1361-6668/ac1aae

Letter

High-temperature superconducting CORC® wires with record-breaking axial tensile strain tolerance present a breakthrough for high-field magnets

D C van der Laan[1,2], K Radcliff[1], V A Anvar[3], K Wang[3], A Nijhuis[3] and J D Weiss[1,2]

[1] Advanced Conductor Technologies LLC, Boulder, CO 80301, United States of America
[2] Department of Physics, University of Colorado, Boulder, CO 80309, United States of America
[3] University of Twente, Enschede, The Netherlands

E-mail: danko@advancedconductor.com

Received 10 May 2021, revised 22 July 2021
Accepted for publication 3 August 2021
Published 13 September 2021

Abstract

Cuprate high-temperature superconductors (HTS), such as RE-$Ba_2Cu_3O_{7-\delta}$ (REBCO, RE = rare earth), $(Bi,Pb)_2Sr_2Ca_2Cu_3O_{10-x}$ and $Bi_2Sr_2CaCu_2O_{8-x}$, have enabled the development of high-field superconducting magnets capable of generating magnetic fields far exceeding 20 T. The brittle nature of HTS requires elaborate means to protect them against the high stresses and strains associated with high-field magnet operation, and so far, has prevented reliable high-field HTS magnets from becoming a reality. Here we report a more than tenfold increase in the irreversible strain limit under axial tension (ε_{irr}) to over 7% in optimized high-current conductor on round core (CORC®) conductors, compared to the REBCO tapes from which the CORC® conductor is wound. Minimizing the tape winding pitch of the helical wind mechanically decouples the brittle REBCO film from the overall conductor. The REBCO tapes behave as springs, limiting the rate at which applied strain is transferred to the ceramic film. In addition, high-strength alloy cores allow the critical stress (ε_{crit}) under axial tension at which initial degradation of CORC® conductors occurs to exceed 600 MPa, making them one of the strongest superconductors available. Mechanically decoupling the ceramic REBCO films from the overall CORC® conductor allows effective protection against the high operating stresses in high-field magnets. This breakthrough presents a monumental shift for HTS magnet technology, bringing reliable high-field superconducting magnets for compact fusion machines, the next generation of particle accelerators, and 40–60 T research solenoids within reach.

Keywords: CORC® cable, high-field superconducting magnets, record irreversible strain limit

(Some figures may appear in color only in the online journal)

1. Introduction

Many large superconducting magnets require conductors capable of operating at high currents of many kilo-amperes with a high engineering current density (J_e) exceeding 300 A mm^{-2}, while having sufficient mechanical strength and strain tolerance to withstand the high stresses that develop during magnet operation. Low-temperature superconducting (LTS) NbTi has been the workhorse of superconducting magnet conductors for many decades because it can be produced in round wires with isotropic magnetic performance and can withstand high tensile strains exceeding 3% [1]. The high

strain tolerance allows winding of fully reacted NbTi wires into magnets without significant loss of performance. The ease of implementing NbTi into magnets has made it the main superconductor serving the commercial markets for superconducting magnets, such as magnetic resonance imaging systems. Intermetallic LTS Nb_3Sn has many of the desired conductor properties of NbTi, while its upper critical field (H_{c2}) of 30 T allows magnet operation to about 22 T at 4.2 K, compared to only 10 T for NbTi with its much lower H_{c2} of 15 T. Nb_3Sn comes with some major challenges that have, until about a decade ago, prevented its widespread application in superconducting magnets. The brittle nature of Nb_3Sn limits ε_{irr}, in terms of applied strain, to less than 0.6% [2]. This requires reaction into the superconducting phase after the magnet has been wound, adding significant cost and risk to the magnet fabrication. The high mechanical operating stresses of large accelerator and fusion magnets require significant operating margins that effectively limit their field to about 15 T when using Nb_3Sn. The higher magnetic field range offered by Nb_3Sn can only be accessed in relatively small solenoids where stresses can be managed more effectively. Nb_3Sn is now being applied more widely in magnets operating at 10–22 T, such as for particle accelerator dipoles in the Large Hadron Collider, high-field nuclear magnetic resonance magnets, and large magnets for fusion machines such as in the International Thermonuclear Experimental Reactor. A growing need has emerged for more powerful research magnets that generate 40–60 T [3, 4], particle accelerator magnets that allow even higher collision energies [5, 6], and compact high-field fusion magnets that have the potential to significantly reduce the time before net fusion energy production becomes a reality [7, 8]. The fundamental limits of LTS make these high-field magnets rely entirely on brittle, poly-crystalline cuprate high-temperature superconductor (HTS), having an H_{c2} of over 100 T at 4.2 K.

The initial challenge of achieving high currents and current densities in poly-crystalline HTS magnet conductors has been largely solved. A high level of grain alignment over the full conductor length is required to prevent the formation of current blocking high-angle grain boundaries [9]. This is achieved in $(Bi,Pb)_2Sr_2Ca_2Cu_3O_{10-x}$ (Bi-2223) by using intermediate rolling steps during formation of the superconducting phase [10]. Sufficient grain connectivity can be introduced into $Bi_2Sr_2CaCu_2O_{8-x}$ (Bi-2212) round wires by reacting them at high pressure up to 10 MPa and high temperature of almost 900° C into the superconducting phase after the magnet is wound [11]. Although very high current densities have been achieved in short Bi-2212 wires, extending the performance from short samples to actual magnets remains highly challenging, adding significant risk and cost to the magnet fabrication process. High-angle grain boundaries are prevented in RE-$Ba_2Cu_3O_{7-\delta}$ (REBCO, RE = rare earth) coated conductors by depositing the superconductor as a highly biaxially aligned thin film onto a metal substrate [12, 13]. The almost single-crystalline films can withstand relatively high axial compressive strains, exceeding −1.2%, while also having the highest ε_{irr} under tension of about 0.6% of any HTS [14, 15], compared to about 0.3% for Bi-2212 wires [16] and 0.4% for Bi-2223 tapes [17].

The brittle nature of HTS restricts their operation to an applied tensile strain of less than 0.3%–0.6%, a far cry from the axial strain of over 3% at which NbTi can operate [1]. The limited strain tolerance of HTS therefore forms the final remaining barrier that prevents practical and reliable high-field magnets from becoming a reality [10–20]. The work presented here outlines how the brittle nature of the REBCO coated conductors can be overcome by mechanically decoupling the REBCO layer from the overall conductor by winding them into composite conductor on round core (CORC®) conductors, in which the REBCO tapes are wound in a helical fashion around a small core [21–24]. Minimizing the helical pitch results in a tenfold increase in ε_{irr} of CORC® conductors with respect to single REBCO tapes. The helical wind does come with a disadvantage in which the high ε_{crit} of single REBCO tapes provided by their strong Hastelloy substrate is not transferred to the composite CORC® conductor [25]. However, incorporating strong cores within the CORC® conductor allows most of the REBCO tape's mechanical strength that was lost due to the helical wind to be regained.

2. CORC® magnet conductors

The relatively high tolerance to axial compressive strain of REBCO coated conductors allows the formation of composite CORC® conductors in which a high number of REBCO tapes are wound in a helical fashion around a small metal core at winding angles (α) ranging from 30° to 50° normal to the CORC® wire axis [21–24] (figure 1). This approach results in a round, fully isotropic (with respect to magnetic field angle and bending direction), high-current conductor that does not require reaction after magnet winding, as desired for many high-field magnet applications, even though the individual REBCO tapes exhibit a highly inhomogeneous in-field performance [26].

CORC® wires have demonstrated in-field performance, with J_e of 450 A mm^{-2} at 20 T [27], sufficient for use in most high-field magnets. This high-field J_e performance achieved in a 3.4 mm diameter CORC® wire is only rivaled by single REBCO tapes and short-sample Bi-2212 wires (figure 2). CORC® conductors have demonstrated a high critical current (I_c) of over 8 kA in combination with a high J_e at fields over 12 T, enabling low-inductance accelerator and compact fusion magnets that allow operation at high ramp rates. The low inductance is a requirement for safe magnet operation, where its stored energy can be extracted quickly in case the superconducting state is suddenly lost. Such a quench results in a rapid formation of a local hot spot and potential conductor burnout if the magnetic energy is not quickly extracted from the magnet.

The helical wind of the REBCO tapes in CORC® conductors also enhances current sharing around defects that may be present in the REBCO layer, resulting in a more stable conductor operation. CORC® conductors allow entering the flux-flow regime at currents exceeding I_c where the superconducting-to-normal transition has started, and significant dissipation occurs. This provides early warning of an

Figure 1. Side view of a CORC® wire.

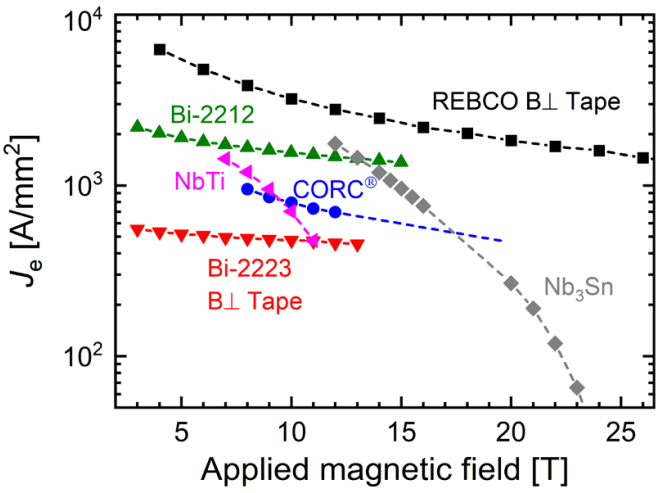

Figure 2. Overall conductor current density as a function of magnetic field at 4.2 K of LTS and HTS magnet conductors. Data for NbTi from [28], Nb_3Sn from [29], Bi-2212 from [30] and CORC® wire from [27]. Data for Bi-2223 from [31] and REBCO tapes from [27] where taken with field applied perpendicular to the tape surface.

imminent magnet quench, which is unheard of in LTS magnets. Entering the flux-flow regime without triggering an immediate quench and returning to the fully superconducting state by reducing the current, has been demonstrated in several prototype high-field magnets such as a canted-cosine-theta accelerator magnet operating at a current of over 6 kA [32, 33], and in a CORC® cable insert solenoid that operated at over 4 kA within a 14 T LTS outsert magnet at a combined magnetic field of 16.77 T [34].

3. Record-level strain limits in CORC® conductors

Contrary to a reversible change in I_c with tensile strain that occurs in most HTS and is driven by the pressure dependence of T_c [17, 35, 36], irreversible degradation in HTS is caused by the formation of cracks in the ceramic material, resulting in permanent degradation to the conductor performance. Such cracks occur in the superconducting film of REBCO coated conductors once the metal substrate yields [14, 15, 37], which is at an applied tensile strain of about 0.6% in REBCO coated conductors with Hastelloy C-276 substrates. Note that the difference in thermal contraction between the metal substrate and the ceramic film causes the film to be in a compressive state after cool-down to cryogenic temperatures of about −0.15%. An applied strain of 0.6% thus corresponds to an intrinsic strain of the REBCO film of 0.45%. The irreversible strain limit is often defined as the applied strain that caused I_c to degrade irreversibly by anywhere between 1% and 3%, depending on the criterion and the sensitivity of the measurement.

The helical wind of REBCO tapes in CORC® conductors prevents the strain applied to the CORC® conductor during magnet operation to be transferred directly to the REBCO tapes [34], similar to how coiled springs behave. The tape's strain state thus increases at a lower rate with applied strain compared to that of a straight tape. The tensile strain of the REBCO tapes within a CORC® conductor depends on the tape's winding angle (α) and Poisson's ratio of the central core, and can be calculated analytically (see inset figure 3):

$$\varepsilon_{\text{tape}} = \frac{\Delta S}{S} = \frac{\frac{l+\Delta l}{\sin\alpha'} - \frac{l}{\sin\alpha}}{\frac{l}{\sin\alpha}} \approx \frac{\Delta l}{l}\left(\sin^2\alpha - \nu\cos^2\alpha\right) \quad (1)$$

here, S is the initial tape length over a full twist pitch, ΔS the change in tape length due to the tape strain $\varepsilon_{\text{tape}}$, while the applied strain of the CORC® wire ε is defined as $\Delta l/l$, with l being the initial twist pitch length before strain is applied. The calculation also takes into account the reduction Δr of the core with axial strain, which is determined by the Poisson's ratio ν of 0.337 in case of copper at cryogenic temperatures [38]. The approach assumes that the radial contraction of the tape spring is limited by the copper core and therefore will closely follow its radius. The torsion component $\Delta\varphi$ can be neglected for tape winding angles below 50°. A more detailed overview of how the strain state of the CORC® wire transfers to the REBCO tape will be provided in a follow-on publication. Figure 3 shows the calculated strain applied to the

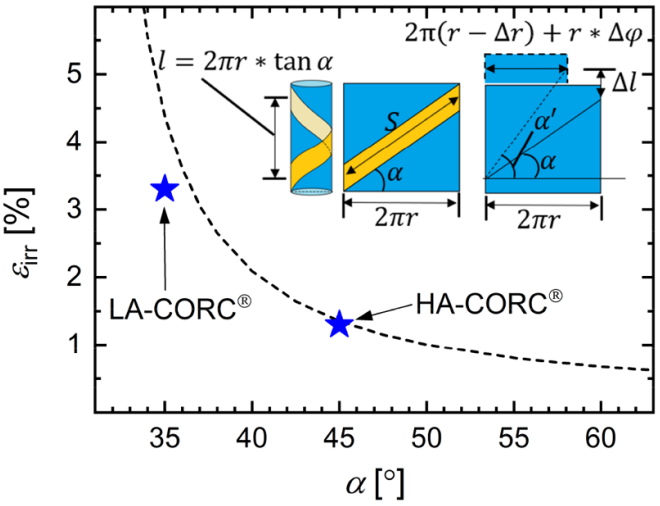

Figure 3. Irreversible tensile strain limit of CORC® wires wound from REBCO tapes as a function of tape winding angle, defined as the angle normal to the CORC® wire axis, calculated using equation (1). The points are the actual irreversible strain limit of 12-tape CORC® wires LA-CORC® and HA-CORC® (see table 1). The trend shows that very high irreversible strains can be achieved by winding the REBCO tapes at a low angle (LA).

Table 1. CORC® wire configuration and performance.

	LA-CORC®	HA-CORC®	CORC®-S30	CORC®-O28
Number of tapes [−]	12	12	30	28
Tape width [mm]	2	2	2	2
Tape layers [−]	6	6	12	14
Core diameter [mm]	2.55	2.55	2.55	2.55
Former material	Cu and CuBe	Cu	Cu	Cu
CORC® thickness [mm]	3.13	3.13	3.67	3.81
Tape winding angle [°]	30–36	40–45	30–47	25–35
Initial I_c (76 K) [A]	828	828	1710	1617
Initial n-value [−]	15–20	15–20	15–20	15–20
ε_{irr} (76 K) [%][a]	3.3	1.5	1.5	>7

[a] Defined at a normalized I_c, $I_c(\varepsilon)/I_c(0) = 0.97$.

CORC® wire with 2.55 mm diameter copper core as a function of tape winding angle at which the strain of the single tape exceeds an applied strain of 0.6%. The irreversible strain limit of the CORC® wire approaches that of the REBCO tape at higher winding angles, while it increases sharply for winding angles below 45°.

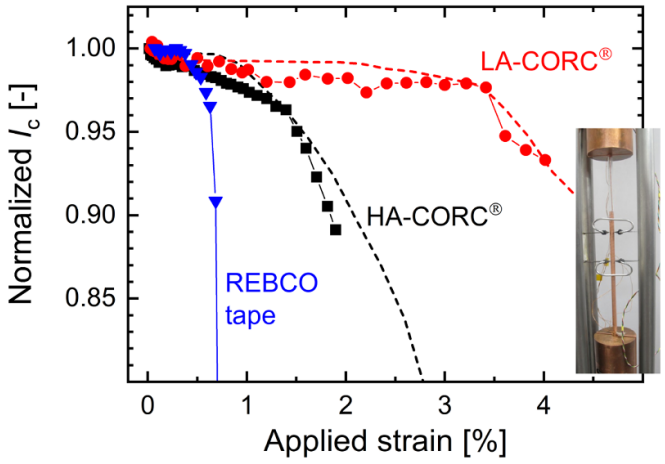

Figure 4. Normalized critical current as a function of applied tensile strain measured in liquid nitrogen of a single REBCO tape [14] and CORC® wires containing 12 tapes wound at angels of 30°–36° (LA-CORC®) and 40°–45° (HA-CORC®). The dashed lines are the dependence of I_c on applied strain determined by finite element method (FEM). The inset shows the double extensometer clamped onto the CORC® wire to measure the applied strain during axial tensile testing.

The hypothesis that ε_{irr} in CORC® conductors depends on the tape winding angle has been confirmed experimentally in CORC® wires with two layouts in which 12 tapes of 2 mm width were wound onto a 2.55 mm diameter copper core at LAs in the range of 30°–36° (LA-CORC®), for which a relatively high ε_{irr} is expected, and at high angles (HA) in the range of 40°–45° (HA-CORC®), for which case ε_{irr} is expected to be relatively low (see table 1). Axial stress was applied in liquid nitrogen by a servo-hydraulic machine connected to the sample terminations, while axial strain was measured by a pair of extensometers clamped directly onto the CORC® wire (inset figure 1). Earlier work in which the performance of CORC® wires under axial tension was measured did not use clamp-on extensometers, but instead relied on the displacement of the servo-hydraulic piston to estimate the CORC® wire strain [25]. The reported ε_{irr} value of 0.85% from [25] therefore needs to be regarded as rough estimate. Figure 4 shows I_c, normalized to its value before strain was applied, as a function of applied axial tensile strain for a CORC® wire of each of the two layouts. The irreversible strain limit of the two CORC® wires increased dramatically compared to that of a single REBCO tape, for which data is included for comparison. Initial degradation of the CORC® wire I_c occurred at an applied strain of about 1.5% when the tapes were wound at angles ranging from 40° to 45°, which is more than twice the ε_{irr} of a straight tape. The irreversible strain limit increased to about 3.3% in the CORC® wire in which the tapes were wound at angles ranging from 30° to 36°. The tapes with the highest winding angle in the CORC® wires are expected to degrade first, which is the tape wound at 45° in sample HA-CORC®, and the tape wound at 36° in sample LA-CORC®. The ε_{irr} of both CORC® wires indeed corresponds closely to the analytical values as indicated in figure 3.

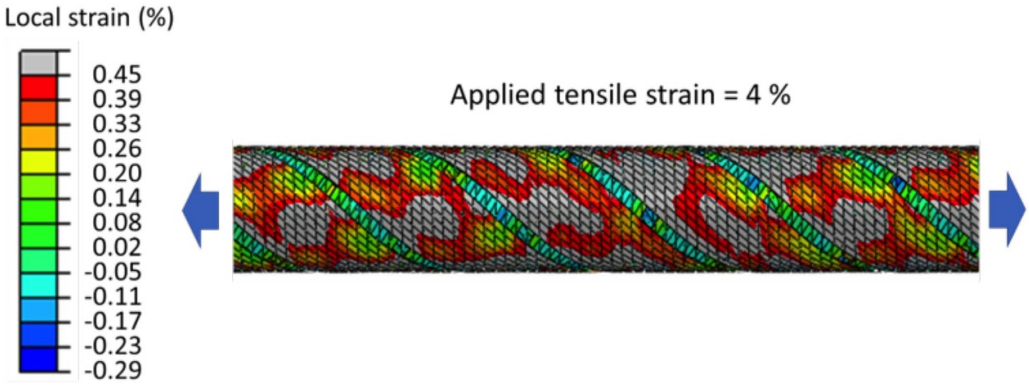

Figure 5. Local strain state within the REBCO coated conductors wound onto the annealed copper core at an angle of 45° with respect to the conductor normal. The applied strain is 4%. Gray areas correspond to the local intrinsic strain of the REBCO layer exceeding 0.45%.

The analytical model assumes that the strain state in the tapes in CORC® wires is homogeneous over the tape width. However, FEM modeling of the local strain state within the tapes shows a clear strain variation over the tape width and along its length, in the case of the layer in which tapes are wound at an angle of 45° (figure 5) [39]. The FEM model takes into account the winding tension of the tapes, and the tension after cool down to cryogenic temperatures. The gray regions in the REBCO film are the locations where a supercurrent can no longer be sustained because the intrinsic strain exceeded 0.45%. Detailed modeling of the local strain distribution within each of the 12 tapes in the CORC® wire allows us to predict the expected I_c of the two CORC® wires, which closely follows the measured I_c as shown in figure 4. The calculation multiplies the initial I_c with the tape surface fraction experiencing a strain above ε_{irr}, while it also considers the reversible change in I_c with strain following the power-law dependence outlined in [14]. Note that the FEM model is solely based on cable geometric and mechanical properties and no fitting factors are applied to match the experimentally measured data.

The dependence of I_c on applied axial tensile strain of a typical high-current 30-tape CORC® wire (CORC®-S30, see table 1) in which the winding angles (30°–47°) are not optimized for high strain tolerance, is shown in figure 6. The CORC® wire has the same layout as the one reported in [25]. The main difference is that in the present case, strain is measured using the clamp-on extensometers, resulting in a much more accurate strain measurement. As mentioned earlier the irreversible strain reported in [25] was 0.85% but a more accurate estimate of 1.5% is obtained with the clamp-on extensometer technique as shown in figure 6. The figure also includes four optimized CORC® wires containing 28 tapes of 2 mm width (CORC®-O28, see table 1) for which the tape winding angles were minimized to 25°–35°. The optimized CORC® wires had an ε_{irr} exceeding 7%, compared to only 1.5% for the 30-tape CORC® wire with standard layout, while both containing a copper former. The results show that ε_{irr} of high-tape count CORC® wires can be improved by almost a factor of 5 by optimizing the winding angles.

A major benefit in the analysis of CORC® conductors is that their REBCO tapes can be extracted from the conductor after strain application, allowing direct performance verification. Figure 7 shows I_c and n-value, which indicates the steepness of the voltage versus current transition, of the 28 REBCO tapes extracted from one of the optimized high-current CORC® wires (CORC®-O28 in figure 6) after the CORC® wire experienced 7% strain. All tapes extracted from the CORC® wire, except for one within the innermost layer of the conductor, maintained their full I_c from before they were cabled and the CORC® wire was strained. The n-values of the tapes also maintained their original value of around 30. The results provide clear evidence that CORC® wires in which the tape winding angles are optimized, can withstand tensile strains as high as 7% without any significant degradation in CORC® wire and tape performance.

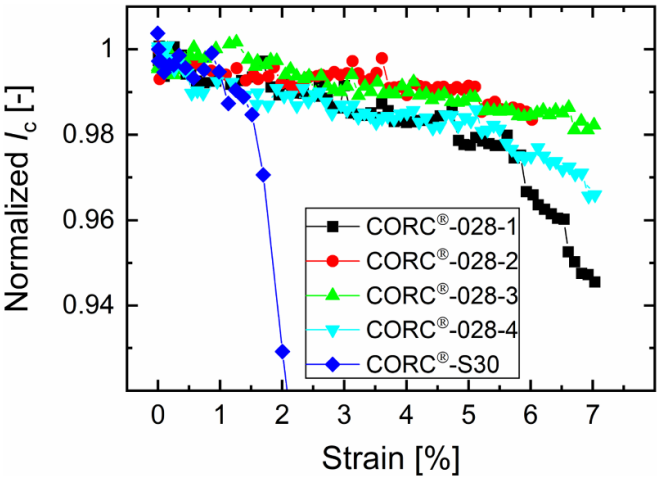

Figure 6. Normalized critical current as a function of applied tensile strain measured in liquid nitrogen of a 30-tape CORC® wire (CORC®-S30) with standard layout (winding angles of 30°–47°) and four optimized 28-tape CORC® wires (CORC®-O28 with winding angles 25°–35°).

4. Increased axial strength in CORC® conductors

The mechanical support provided by the Hastelloy substrate results in a ε_{crit} of over 1 GPa at 77 K in straight REBCO

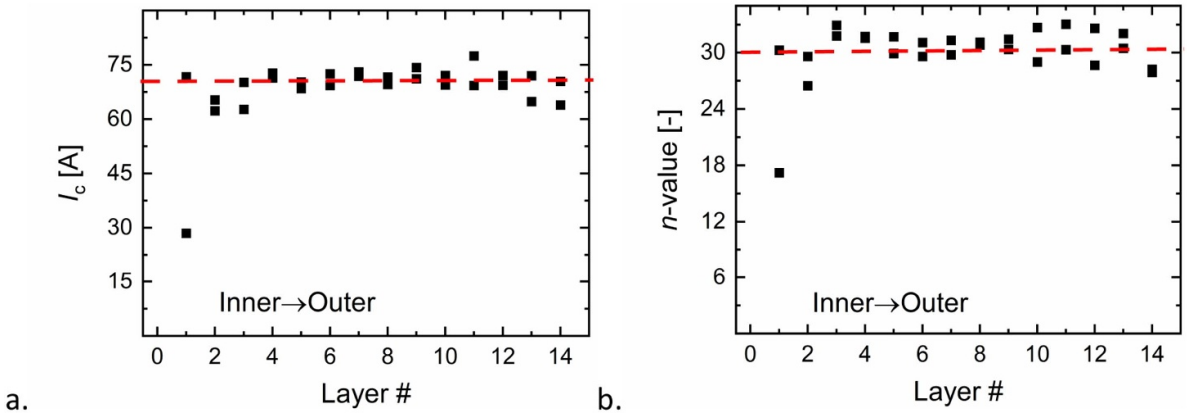

Figure 7. (a) I_c and (b) n-value of REBCO tapes extracted from an optimized 28-tape CORC® wire (CORC®-O28) after being strained to 7% plotted as a function of layer number (position within the conductor). Measurements were performed in liquid nitrogen.

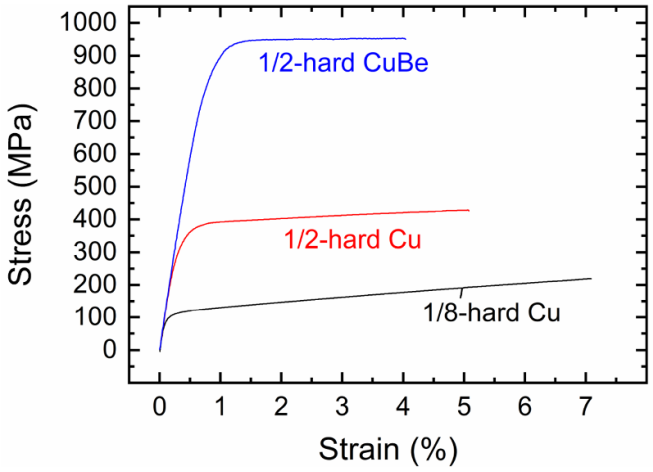

Figure 8. Stress as a function of tensile strain measured in liquid nitrogen of copper (1/8 and 1/2 hard) and copper–beryllium (1/2 hard) formers.

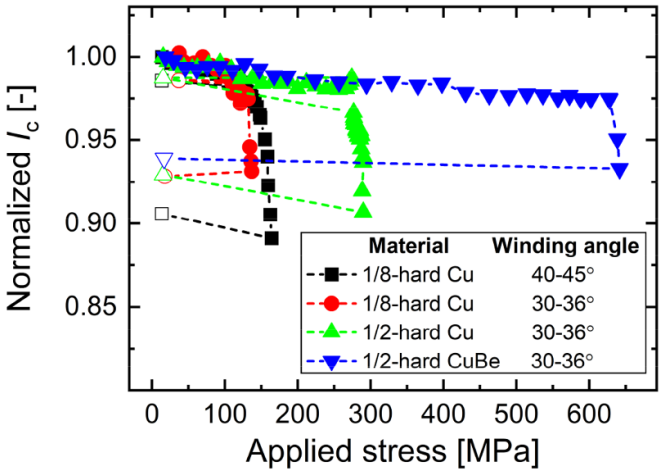

Figure 9. Normalized critical current of HTS CORC® wires containing various metal cores as a function of tensile stress in liquid nitrogen, showing a significant increase in critical stress can be achieved by using stronger materials. The open symbols show that I_c recovers by 1%–2% after the load is removed.

coated conductors but is mostly lost when winding the tapes in a helical fashion into CORC® conductors [25]. Mechanical strength instead needs to be provided by the metal core onto which the tapes are wound. Figure 8 shows the stress versus strain characteristic measured in liquid nitrogen of two copper formers with yield strength 114 and 363 MPa for 1/8 and 1/2 hard copper respectively, and a 1/2 hard CuBe former with yield strength 872 MPa. Figure 9 compares the dependence of I_c in liquid nitrogen on applied tensile stress of CORC® wires with various metal cores. CORC® wires containing a 2.55 mm diameter half-hard copper core have a ε_{crit} of close to 300 MPa at 77 K, compared to about 130 MPa when using softer eighth-hard copper cores, while it exceeds 600 MPa for a 12-tape CORC® wire containing a CuBe core. The initial slope of I_c below ε_{crit} originates from the reversible change in the REBCO tape I_c with strain [14] and is not caused by crack formation, as is evident when I_c partly recovers after the load is removed (open symbols in figure 9).

5. A breakthrough for high-field magnets

Round isotropic high-temperature superconductors are often seen as the most desirable topology for use in high-field magnets [11]. REBCO-based CORC® conductors, besides offering such desirable topology, allow the ceramic REBCO film of the tapes to be decoupled mechanically from the overall conductor, resulting in more than a tenfold increase of ε_{irr} compared to that of the straight REBCO tapes. The impact of this innovation becomes even more evident when comparing ε_{irr} of optimized CORC® wires to that of most other LTS and HTS magnet conductors, where it is 10–20 times higher than ε_{irr} of Bi-2223, Bi-2212, REBCO and Nb_3Sn, and even more than twice the ε_{irr} of NbTi (figure 10). The CORC® conductor topology separates the components driving the conductor's critical stress from those that make it strain tolerant. Low tape winding angles in combination with strong

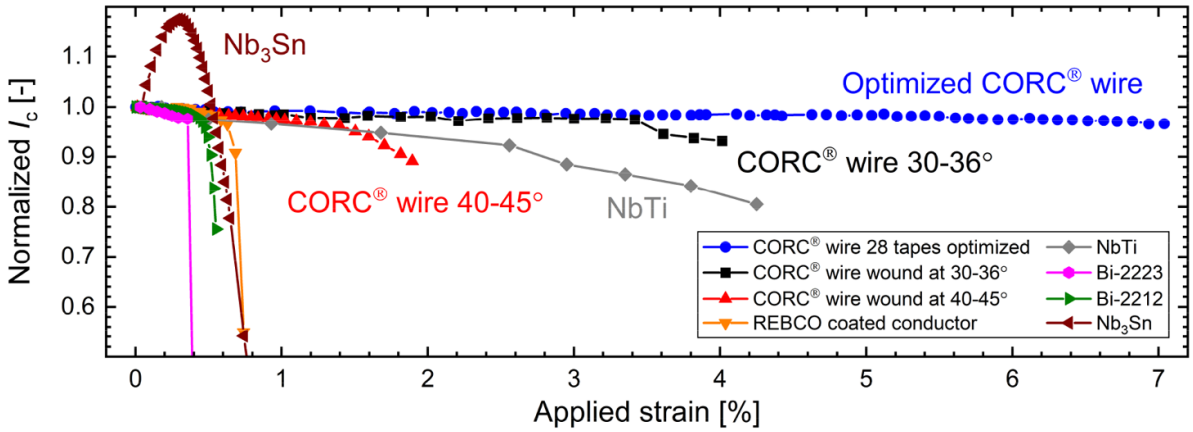

Figure 10. Normalized critical current as a function of applied axial tensile strain of most practical LTS and HTS superconductors. Data is taken in liquid nitrogen in case of Bi-2223, REBCO coated conductors and CORC® wires, and in liquid helium in case of Bi-2212, NbTi and Nb_3Sn. Bi-2212 from [16], Nb_3Sn data from [2], and Nb-Ti data from [1], REBCO coated conductor data from [14], and Bi-2223 tape data from [17].

elastic cores allow the best of both worlds, providing the conductor with high critical stress while making it highly strain tolerant.

The breakthrough reported here would certainly have a major impact on the development and implementation of reliable HTS high-field magnets. The high strain tolerance of HTS CORC® conductors significantly eases the design and construction of high-field magnets, where the conductor strain state during magnet operation no longer needs to be kept within a highly restricted range to prevent conductor degradation. The high stresses and strains that occur during a magnet quench have caused many of the prototype HTS magnets to fail. Strain tolerant, high-strength CORC® conductors may experience only minor effects of a magnet quench and thus have the potential of providing high-field superconducting magnets with the reliability required for the many applications that rely on them.

Data availability statement

The data that support the findings of this study are available upon reasonable request from the authors.

Acknowledgments

This material is based upon work supported by the U S Department of Energy, Office of Science, Offices of High Energy Physics and Fusion Energy Sciences, under Award Numbers DE-SC0014009, DE-SC0018125 and DE-SC0020710. Part of this work has been carried out within the framework of the EUROfusion Consortium and has received funding from the EURATOM Research and Training Program 2014–2018. The views and opinions expressed herein do not necessarily reflect those of the European Commission.

ORCID iDs

D C van der Laan https://orcid.org/0000-0001-5889-3751
A Nijhuis https://orcid.org/0000-0002-1600-9451

References

[1] Ekin J W 1977 Mechanisms for critical current degradation in NbTi and Nb_3Sn multifilamentary wires *IEEE Trans. Magn.* **13** 127–30
[2] Najib Cheggour T C, Stauffer W S, Lee P J, Splett J D, Goodrich L F and Ghosh A K 2018 Precipitous change of the irreversible strain limit with heat treatment temperature in Nb_3Sn wires made by the restacked-rod process *Sci. Rep.* **8** 13048
[3] Pugnat P and Schneider-Muntau H J 2020 Conceptual design optimization of a 60 T hybrid magnet *IEEE Trans. Appl. Supercond.* **30** 4300507
[4] Bai H *et al* 2020 The 40 T superconducting magnet project at the national high magnetic field laboratory *IEEE Trans. Appl. Supercond.* **30** 4300405
[5] Rossi L *et al* 2015 The EuCARD-2 future magnets European collaboration for accelerator-quality HTS magnets *IEEE Trans. Appl. Supercond.* **25** 4001007
[6] Prestemon S, Amm K, Cooley L, Gourlay S, Larbalestier D, Velev G and Zlobin A 2020 The 2020 updated roadmaps for the US Magnet Development Program (available at: https://science.osti.gov/-/media/hep/pdf/Reports/2020/USMDP-2020-Plan-Update-web.pdf?la=en%26hash=CDF960B4B079A4182F024B159C87EF528B33B2C0) (August 11, 2021)
[7] Sorbom B N *et al* 2015 ARC: a compact, high-field, fusion nuclear science facility and demonstration power plant with demountable magnets *Fusion Eng. Des.* **100** 378–405
[8] Sykes A *et al* 2018 Compact fusion energy based on the spherical tokamak *Nucl. Fusion* **58** 016039
[9] Hilgenkamp H and Mannhart J 2002 Grain boundaries in high-T_c superconductors *Rev. Mod. Phys.* **74** 485–549
[10] Rupich M W and Hellstrom E E 2011 *One Hundred Years of Superconductivity Rogalla Horst* and Kes Peter (CRC Press/Taylor & Francis) pp 671–89

[11] Larbalestier D C *et al* 2014 Isotropic round-wire multifilament cuprate superconductor for generation of magnetic fields above 30 T *Nat. Mater.* **13** 375–81

[12] Iljima Y, Tanabe N, Kohno O and Ikeno Y 1992 In-plane aligned $YBa_2Cu_3O_{7-x}$ thin-films deposited on polycrystalline metallic substrates *Appl. Phys. Lett.* **60** 769–71

[13] Goyal A *et al* 1996 High critical current density superconducting tapes by epitaxial deposition of $YBa_2Cu_3O_x$ thick films on biaxially textured metals *Appl. Phys. Lett.* **69** 1795–7

[14] van der Laan D C and Ekin J W 2007 Large intrinsic effect of axial strain on the critical current of high temperature superconductors for electric power applications *Appl. Phys. Lett.* **90** 052506

[15] Zhang Y, Hazelton D W, Kelley R, Kasahara M, Nakasaki R, Sakamoto H and Polyanskii A 2016 Stress–strain relationship, critical strain (stress) and irreversible strain (stress) of IBAD-MOCVD-based 2G HTS wires under uniaxial tension *IEEE Trans. Appl. Supercond.* **26** 8400406

[16] Cheggour N, Lu X F, Holesinger T G, Stauffer T C, Jiang J and Goodrich L F 2012 Reversible effect of strain on transport critical current in $Bi_2Sr_2CaCu_2O_{8+x}$ superconducting wires: a modified descriptive strain model *Supercond. Sci. Technol.* **25** 015001

[17] van der Laan D C, Douglas J F, Clickner C C, Stauffer T C, Goodrich L F and van Eck H J N 2011 Evidence that the reversible strain effect on critical current density and flux pinning in $Bi_2Sr_2Ca_2Cu_3O_x$ tapes is caused entirely by the pressure dependence of the critical temperature *Supercond. Sci. Technol.* **24** 032001

[18] van Nugteren J *et al* 2018 Powering of an HTS dipole insert-magnet operated standalone in helium gas between 5 and 85 K *Supercond. Sci. Technol.* **31** 065002

[19] Bird M D, Bai H, Dixon I R and Gavrilin A V 2019 Test results of the 36 T, 1 ppm series-connected hybrid magnet system at the NHMFL *IEEE Trans. Appl. Supercond.* **29** 4300105

[20] Hahn S *et al* 2019 45.5-tesla direct-current magnetic field generated with a high-temperature superconducting magnet *Nature* **570** 496–9

[21] van der Laan D C 2009 $YBa_2Cu_3O_{7-\delta}$ coated conductor cabling for low ac-loss and high-field magnet applications *Supercond. Sci. Technol.* **22** 065013

[22] van der Laan D C, Noyes P D, Miller G E, Weijers H W and Willering G P 2013 Weijers H W and Willering G P, 'Characterization of high-temperature superconducting conductor on round core cables in magnetic fields up to 20 teslas' *Supercond. Sci. Technol.* **26** 045005

[23] Weiss J D, Mulder T, Ten Kate H J J and van der Laan D C 2017 Introduction of CORC® wires: highly flexible, round high-temperature superconducting wires for magnet and power transmission applications *Supercond. Sci. Technol.* **30** 014002

[24] van der Laan D C, Weiss J D and McRae D M 2019 Status of CORC® cables and wires for use in high-field magnets and power systems a decade after their introduction *Supercond. Sci. Technol.* **32** 033001

[25] van der Laan D C, McRae D M and Weiss J D 2019 Effect of monotonic and cyclic axial tensile stress on the performance of superconducting CORC® wires *Supercond. Sci. Technol.* **32** 054004

[26] Civale L *et al* 2004 Angular dependent vortex pinning mechanisms in YBCO coated conductors and thin films *Appl. Phys. Lett.* **84** 2121–3

[27] Weiss J D, van der Laan D C, Hazelton D, Knoll A, Carota G, Abraimov D, Francis A, Small M A, Bradford G and Jaroszynski J 2020 Introduction of the next generation of CORC® wires with engineering current density exceeding 650 A mm^{-2} at 12 T based on SuperPower's ReBCO tapes containing substrates of 25 μm thickness *Supercond. Sci. Technol.* **33** 044001

[28] Boutboul T, Le Naour S, Leroy D, Oberli L and Previtali V 2006 Critical current density in superconducting NbTi strands in the 100 mT to 11 T applied field range *IEEE Trans. Appl. Supercond.* **16** 1184–7

[29] Parrell J A, Youzhu Zhang M B, Field P C and Hong S 2003 High field Nb_3Sn conductor development at Oxford Superconducting Technology *IEEE Trans. Appl. Supercond.* **13** 3470–3

[30] Jiang J *et al* 2019 High-performance Bi-2212 round wires made with recent powders *IEEE Trans. Appl. Supercond.* **29** 6400405

[31] Abraimov D, Private communications (available at: https://nationalmaglab.org/magnet-development/applied-superconductivity-center) (August 11, 2021)

[32] Wang X, Dietderich D R, DiMarco J, Ghiorso W B, Gourlay S S A, Higley H C, Lin A, Prestemon S O, van der Laan D C and Weiss J D 2019 A 1.2 T canted cosθ dipole magnet using high-temperature superconducting CORC® wires *Supercond. Sci. Technol.* **32** 075002

[33] Wang X *et al* 2021 Development and performance of a 2.9 Tesla dipole magnet using high-temperature superconducting CORC® wires *Supercond. Sci. Technol.* **34** 015012

[34] van der Laan D C *et al* 2020 A CORC® cable insert solenoid: the first high-temperature superconducting insert magnet tested at currents exceeding 4 kA in 14 T background magnetic field *Supercond. Sci. Technol.* **33** 05LT03

[35] van der Laan D C, Abraimov D, Polyanskii A A, Larbalestier D C, Douglas J F, Semerad R and Bauer M 2011 Anisotropic in-plane reversible strain effect in $Y_{0.5}Gd_{0.5}Ba_2Cu_3O_{7-\delta}$ coated conductors *Supercond. Sci. Technol.* **24** 115010

[36] Lu X F, Goodrich L F, van der Laan D C, Splett J D, Cheggour N, Holesinger T G and Baca F 2012 Correlation between the pressure dependence of the critical temperature and the reversible strain effect on the critical current and pinning force in $Bi_2Sr_2CaCu_2O_{8+x}$ wires *IEEE Trans. Appl. Supercond.* **22** 8400307

[37] Zhou C, Yagotintsev K A, Gao P, Haugan T J, van der Laan D C and Nijhuis A 2016 Critical current of various REBCO tapes under uniaxial strain *IEEE Trans. Appl. Supercond.* **26** 7420668

[38] Reed R P and Mikesell R P 1967 Low temperature mechanical properties of copper and selected copper alloys *NBS Monograph* vol 101 (Boulder, Colorado: Institute for Materials Research, National Bureau of Standards) p 80302

[39] Ilin K, Yagotintsev K A, Zhou C, Gao P, Kosse J, Otten S J, Wessel W A J, Haugan T J, van der Laan D C and Nijhuis A 2015 Experiments and FE modeling of stress–strain state in ReBCO tape under tensile, torsional and transverse load *Supercond. Sci. Technol.* **28** 055006